

Characterization of Physical, Spectral and Thermal Properties of Biofield Treated 1,2,4-Triazole

Mahendra Kumar Trivedi¹, Rama Mohan Tallapragada¹, Alice Branton¹, Dahryn Trivedi¹, Gopal Nayak¹, Rakesh Kumar Mishra² and Snehasis Jana^{2*}

¹Trivedi Global Inc., 10624 S Eastern Avenue Suite A-969, Henderson, NV 89052, USA

²Trivedi Science Research Laboratory Pvt. Ltd., Hall-A, Chinar Mega Mall, Chinar Fortune City, Hoshangabad Rd., Bhopal-462026, Madhya Pradesh, India

Abstract

Triazoles are an important class of compounds used as core molecule for the synthesis of many pharmaceutical drugs. The objective of the present research was to investigate the influence of biofield treatment on physical, spectral and thermal properties of 1,2,4-triazole. The study was performed in two groups, control and treatment. The control group remained as untreated, and biofield treatment was given to treatment group. The control and treated 1,2,4-triazole were characterized by X-ray diffraction (XRD), Differential Scanning Calorimetry (DSC), Thermo Gravimetric analysis (TGA), Surface area analyzer, and Fourier transform infrared (FT-IR) spectroscopy. XRD analysis revealed a decrease in unit cell volume of treated 1,2,4-triazole ($662.08 \times 10^{-24} \text{ cm}^3$) as compared to control sample ($666.34 \times 10^{-24} \text{ cm}^3$). Similarly, a decrease in molecular weight of treated 1,2,4-triazole (69.78 g/mol) with respect to control (70.23 g/mol) was observed. Additionally, a substantial decrease in crystallite size (G) was observed in treated 1,2,4-triazole by 16.34% with respect to control. DSC analysis showed a slight increase in melting temperature of treated 1,2,4-triazole (124.22°C) as compared to control (123.76°C). Moreover, a significant increase in latent heat of fusion was noticed in treated 1,2,4-triazole by 21.16% as compared to control sample. TGA analysis showed a significant increase in maximum thermal decomposition temperature (T_{max}) of treated 1,2,4-triazole (213.40°C) as compared to control (199.68°C). Surface area analysis using BET showed a substantial increase in surface area of the treated compound by 13.52% with respect to control. However, FT-IR analysis showed no structural changes in treated 1,2,4-triazole with respect to control. Overall, the result showed significant alteration of physical and thermal properties of the treated 1,2,4-triazole with respect to control.

Keywords: Biofield treatment; 1,2,4-Triazole; X-ray diffraction; Differential scanning calorimetry; Thermo gravimetric analysis; Surface area analyzer; Fourier transform infrared spectroscopy

Abbreviations: XRD: X-Ray Diffraction; DSC: Differential Scanning Calorimetry; TGA: Thermo Gravimetric Analysis; FT-IR: Fourier Transform Infrared.

Introduction

Now-a-days research is focused towards the introduction of novel and biologically safe therapeutic agents. Recently nitrogen-containing heterocycles are commonly found in most of the medicinal compounds. Triazoles are fused heterocyclic compounds that have received considerable attention owing to their synthetic and medicinal importance. Especially, 1,2,4-triazole was used as core molecule for the synthesis of different pharmacological agents such as anti-inflammatory, CNS stimulants, sedative, anti-anxiety, antimicrobial, and anti-migraine activity [1]. 1,2,4-Triazole derivatives have received considerable attention as antifungal agents such as fluconazole and itraconazole [2-4]. These compounds have advantages due to its low toxicity, high oral bioavailability and a broad spectrum of activity against several fungi [5-7]. Kurtzer, et al. reported that 4-amino-5-mercapto-3-substituted-1,2,4-triazole compound has excellent antifungal, anti-inflammatory and anti-tubercular activities that make them potential chemotherapeutic agents [8].

The chemical and physical stability of the pharmaceutical compounds are more desired quality attributes that directly affect its safety, efficacy, and shelf life [9]. Hence, it is required to explore some new alternate approach that could alter the physical and chemical properties of the compounds. Mohammadi et al. used fast neutron and gamma irradiation to investigate the thermal, structural and physical properties of an organic compound [10]. Recently biofield treatment

was used as an excellent strategy for modification of spectral properties of various pharmaceutical drugs like paracetamol, piroxicam, and physicochemical properties of metals, beef extract, and meat infusion powder [11-13].

Recently it was discovered that electrical process occurring in the human body has a relation with the magnetic field. Rivera-Ruiz et al. reported that electrocardiography has been extensively used to measure the biofield of the human body [14]. According to Ampere's law, the moving charge produces the magnetic field in surrounding space. Likewise, human body emits the electromagnetic waves in the form of bio-photons, which surrounds the body, and it is commonly known as biofield. Therefore, the biofield consists of an electromagnetic field, being generated by moving electrically charged particles (ions, cell, molecule, etc.) inside the human body. Thus, human beings have the ability to harness the energy from environment/Universe and can transmit into any object (living or non-living) around the Globe. The object(s) always receive the energy and responding in a useful manner that is called biofield energy. Mr. Trivedi's unique biofield treatment

***Corresponding author:** Jana S, Trivedi Science Research Laboratory Pvt. Ltd., Hall-A, Chinar Mega Mall, Chinar Fortune City, Hoshangabad Rd., Bhopal 462026, Madhya Pradesh, India, Tel: +91-755-6660006; E-mail: publication@trivedisrl.com

Received August 17, 2015; Accepted August 29, 2015; Published August 31, 2015

Citation: Trivedi MK, Tallapragada RM, Branton A, Trivedi D, Nayak G, et al. (2015) Characterization of Physical, Spectral and Thermal Properties of Biofield Treated 1,2,4-Triazole. J Mol Pharm Org Process Res 3: 128. doi:10.4172/2329-9053.1000128

Copyright: © 2015 Trivedi MK, et al. This is an open-access article distributed under the terms of the Creative Commons Attribution License, which permits unrestricted use, distribution, and reproduction in any medium, provided the original author and source are credited.

is also known as The Trivedi Effect®. Mr. Trivedi biofield treatment is known to transform the characteristics of various living and nonliving things. The biofield treatment has improved the growth and production of agriculture crops [15-18] and significantly altered the phenotypic characteristics of various pathogenic microbes [19-21]. Additionally, biofield treatment has substantially altered the medicinal, growth and anatomical properties of ashwagandha [22].

Based on the excellent outcome from biofield treatment and interesting pharmaceutical applications of 1,2,4-Triazole, this work was undertaken to investigate the impact of biofield treatment on this compound.

Materials and Methods

1,2,4-triazole was procured from SD Fine Chemicals Limited, India. The sample was divided into two parts; one was kept as a control sample while the treatment group (T) was in sealed pack and handed over to Mr. Trivedi for biofield treatment under laboratory condition. Mr. Trivedi provided the treatment through his energy transmission process to the treated group without touching the sample. The control and treated samples were characterized by XRD, DSC, TGA, surface area analysis, and FT-IR.

Characterization

X-ray diffraction (XRD) study

XRD analysis of control and treated 1,2,4-triazole was carried out on Phillips, Holland PW 1710 X-ray diffractometer system, which had a copper anode with nickel filter. The radiation of wavelength used by the XRD system was 1.54056 Å. The data obtained from this XRD were in the form of a chart of 2θ vs. intensity and a detailed table containing peak intensity counts, d value (Å), peak width (θ°), relative intensity (%) etc. The crystallite size (G) was calculated by using formula:

$$G = k\lambda / (b\cos\theta)$$

Here, λ is the wavelength of radiation used, b is full width half-maximum (FWHM) of peaks and k is the equipment constant (=0.94). Percent change in unit cell volume was calculated using following formula

$$\text{Percent change in unit cell volume} = \left[\frac{(V_t - V_c)}{V_c} \right] \times 100$$

The molecular weight of atom was calculated using following equation:

Molecular weight = number of protons x weight of a proton + number of neutrons x weight of a neutron + number of electrons x weight of an electron.

Molecular weight in g/mol was calculated from the weights of all atoms in a molecule multiplied by the Avogadro number (6.023×10^{23}). The percent change in molecular weight was calculated using the following equation:

$$\text{Percent change in molecular weight} = \left[\frac{(M_t - M_c)}{M_c} \right] \times 100$$

Where, M_c and M_t are molecular weight of control and treated powder sample respectively

Percentage change in crystallite size was calculated using following formula:

$$\text{Percentage change in crystallite size} = \left[\frac{(G_t - G_c)}{G_c} \right] \times 100$$

Where, G_c and G_t are crystallite size of control and treated powder

samples respectively.

Differential Scanning Calorimetry (DSC)

DSC was used to investigate the melting temperature and latent heat of fusion (ΔH) of samples. The control and treated 1,2,4-triazole samples were analyzed using a Pyris-6 Perkin Elmer DSC on a heating rate of $10^\circ\text{C}/\text{min}$ under air atmosphere and air was flushed at a flow rate of $5 \text{ mL}/\text{min}$. The sample was kept in an aluminum pan and covered with a lid. Another blank covered aluminum pan was used as reference in the study.

Percentage change in latent heat of fusion was calculated using following equations:

$$\% \text{ change in Latent heat of fusion} = \frac{[\Delta H_{\text{Treated}} - \Delta H_{\text{Control}}]}{\Delta H_{\text{Control}}} \times 100$$

Where, $\Delta H_{\text{Control}}$ and $\Delta H_{\text{Treated}}$ are the latent heat of fusion of control and treated samples, respectively.

Thermo Gravimetric Analysis-Differential Thermal Analysis (TGA-DTA)

Thermal stability of control and treated 1,2,4-triazole were analyzed by using Mettler Toledo simultaneous TGA and Differential thermal analyzer (DTA). The samples were heated from room temperature to 400°C with a heating rate of $5^\circ\text{C}/\text{min}$ under air atmosphere.

Percent change in temperature at which maximum weight loss occur in sample was calculated using following equation:

$$\% \text{ change in } T_{\text{max}} = \left[\frac{(T_{\text{max, treated}} - T_{\text{max, control}})}{T_{\text{max, control}}} \right] \times 100$$

Where, $T_{\text{max, control}}$ and $T_{\text{max, treated}}$ are the maximum thermal decomposition temperature in control and treated sample, respectively.

Surface area analysis

Surface area of 1,2,4-triazole were characterized by surface area analyzer, SMART SORB 90 Brunauer-Emmett-Teller (BET) using ASTM D 5604 method which had a detection range of $0.2-1000 \text{ m}^2/\text{g}$. Percent changes in surface area were calculated using following equation:

$$\% \text{ change in surface area} = \frac{[S_{\text{Treated}} - S_{\text{Control}}]}{S_{\text{Control}}} \times 100$$

Where, S_{Control} and S_{Treated} are the surface area of control and treated samples respectively.

FT-IR spectroscopy

FT-IR spectra were recorded on Shimadzu's Fourier transform infrared spectrometer (Japan) with frequency range of $4000-500 \text{ cm}^{-1}$. The treated sample was divided in two parts T1 and T2 for FT-IR analysis.

Results and Discussions

XRD study

XRD diffractograms of control and treated 1,2,4-triazole are shown in Figure 1.

XRD diffractogram of control 1,2,4-triazole showed intense crystalline peaks at 2θ equal to 17.91° , 22.23° , 22.41° , 22.57° , 24.40° ,

24.67°, 26.16°, 26.40°, 27.74°, 28.10°, 31.14°, 32.34°, 32.54°, 54.70° and 54.86°. Similarly, the treated 1,2,4-triazole showed crystalline peaks at 2θ equal to 18.00°, 18.20°, 18.97°, 22.26°, 22.44°, 22.65°, 23.77°, 24.42°, 24.70°, 26.21°, 26.37°, 28.12° and 31.32°. The result showed that few XRD peaks of control 1,2,4-triazole originally present at 2θ equal to 22.57°, 24.67° and 28.10° were shifted to 22.65°, 24.70° and 28.12° respectively, in treated sample. Moreover, the intensity was significantly increased for these XRD peaks of treated 1,2,4-triazole as compared to control, indicating an increase in crystallinity (Figure 1). It is hypothesized that biofield treatment may cause the formation of the long-range order of treated 1,2,4-triazole molecules which leads to increase in crystallinity with respect to control. Based on the XRD data of control and treated 1,2,4-triazole the crystal structure was orthorhombic.

The unit cell volume, molecular weight and crystallite size of control and treated 1,2,4-triazole were computed from the respective XRD diffractogram and data are depicted in Table 1.

The unit cell volume of control 1,2,4-triazole was $666.34 \times 10^{-24} \text{ cm}^3$; however it was decreased slightly to $662.08 \times 10^{-24} \text{ cm}^3$ in treated sample. The decrease in volume of unit cell volume was 0.64% as compared to control. It is assumed that compressive stress may applied due to biofield treatment that decreases the parameter and unit cell volume. Whereas the molecular weight of control 1,2,4-triazole was decreased by 0.64% with respect to control. It is speculated that biofield may cause

an alteration in proton to neutron ratio in the treated 1,2,4-triazole that leads to a reduction in molecular weight.

The crystallite size of control and treated 1,2,4-triazole were computed from the Scherrer formula ($\text{crystallite size} = k\lambda / b \cos \theta$) and presented in Figure 2.

The crystallite size of control 1,2,4-triazole was 84.36 nm and it was decreased to 70.58 nm in treated 1,2,4-triazole. The result showed a decrease in crystallite size of biofield treated 1,2,4-triazole by 16.33% with respect to control. Researchers have reported that ball milling and similar other treatment methods cause a substantial decrease in grain size and crystallite size of materials [23]. Suryanarayana reported that crystallite size/grain size decreases rapidly in early stages of milling and then slowly reaches a few nanometers in a short time [24]. Previously it was reported that biofield treatment had substantially reduced the crystallite size of vanadium pentoxide powders [25]. Hence, it is assumed that biofield treatment may provide energy milling to the treated 1,2,4-triazole samples that lead the creation of linear defects particularly dislocations which results in higher dislocation density and decrease in crystallite size [23].

DSC study

DSC was used to study the latent heat of fusion and melting behavior of the 1,2,4-triazole. Figure 3 showed the DSC thermogram of control and treated 1,2,4-triazole. DSC thermogram of control 1,2,4-triazole showed a sharp endothermic peak at 123.76°C. However the treated

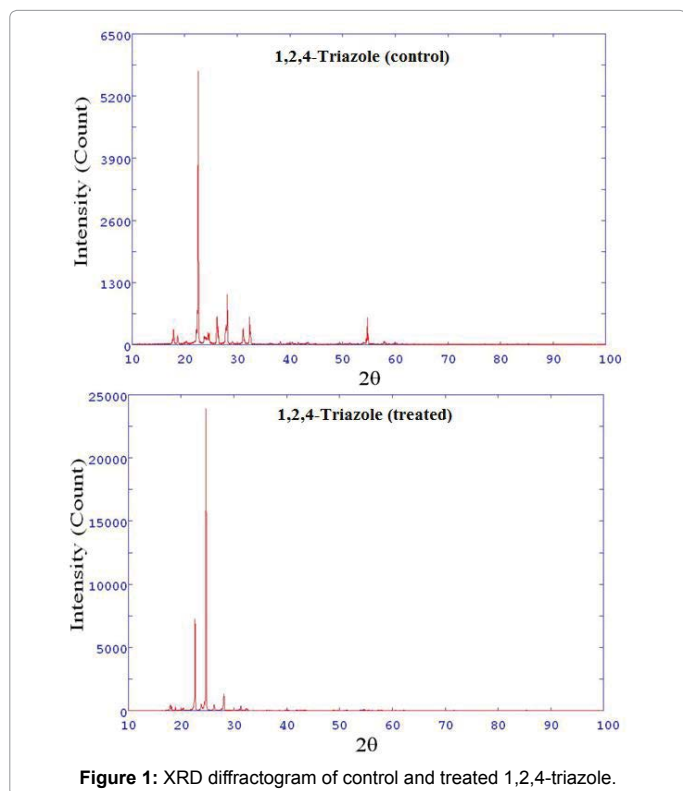


Figure 1: XRD diffractogram of control and treated 1,2,4-triazole.

Compound Characteristics	Control	Treated
Unit cell volume (10^{-24} cm^3)	666.34	662.08
Molecular weight (g/mol)	70.23	69.78

Table 1: XRD data (unit cell volume, crystallite size and molecular weight) of control and treated 1,2,4-triazole.

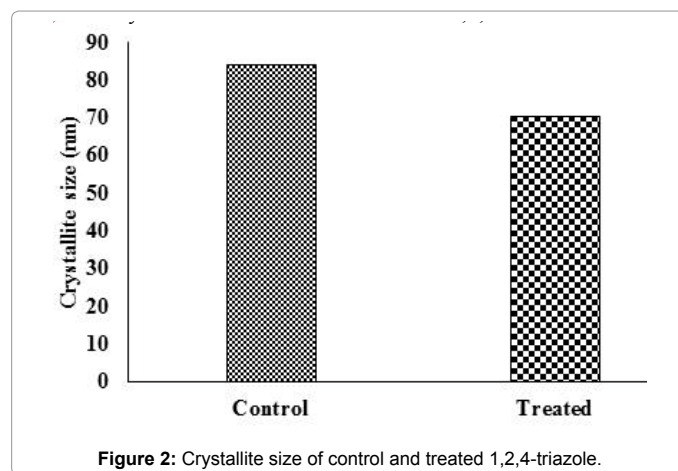


Figure 2: Crystallite size of control and treated 1,2,4-triazole.

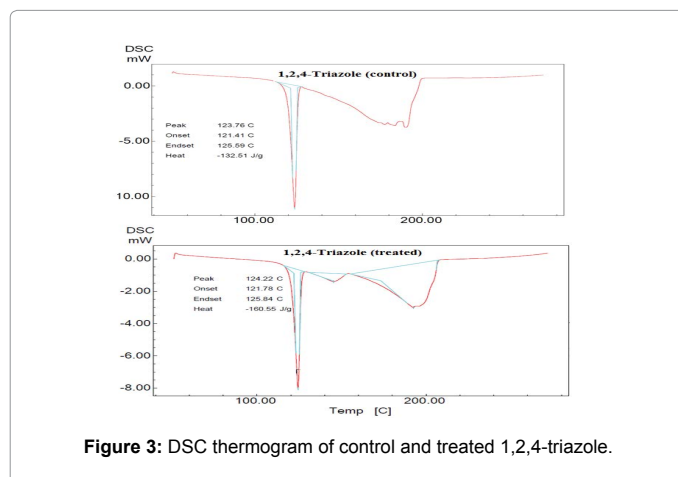


Figure 3: DSC thermogram of control and treated 1,2,4-triazole.

1,2,4-triazole showed an intense endothermic peak at 124.22°C, corresponded to melting temperature of the sample (Figure 3).

This showed a slight increase in melting temperature of the biofield treated sample with respect to control. When molecules come out from the regular pattern of the material and starts to vibrate thermally, that is known as melting temperature. Researchers have showed that melting temperature of a material depends on its kinetic energy [26]. It is assumed that biofield treatment may altered the kinetic energy of the treated 1,2,4-triazole that leads to a slight increase in melting temperature with respect to control.

Latent heat of fusion of control and treated 1,2,4-triazole were computed from the respective thermograms and data are reported in Table 2.

It was suggested that a material consist of strong intermolecular forces between them that holds them tightly on their positions. The energy needed to overcome this strong intermolecular force is known as latent heat of fusion. This latent heat of fusion is stored as potential energy in the atoms during its phase transition from solid to liquid. The control sample showed a latent heat of fusion of 132.51 J/g and it was considerably increased in treated 1,2,4-triazole (160.55 J/g). The result showed a significant increase in latent heat of fusion by 21.16% with respect to the control sample. It is speculated that biofield treatment may alter the stored potential energy in the sample that leads to increase in latent heat of fusion of the sample.

TGA analysis

Thermo gravimetric analysis is a technique used to evaluate the thermal stability, vaporization and sublimation of the sample. TGA thermogram of control and treated 1,2,4-triazole are presented in Figure 4.

The control 1,2,4-triazole started to degrade thermally around 186°C (onset), and it stopped at around 226°C (end set). During this process, the sample lost 53.79% of its weight. However, the treated 1,2,4-triazole started to thermally decompose at 200°C (onset), and it terminated at around 243°C (end set). The sample lost 50.71% of its weight during this process. This showed an increase in onset temperature of treated 1,2,4-triazole with respect to the control sample. This may be inferred as high thermal stability of treated 1,2,4-triazole with respect to control.

DTA thermogram of control and treated 1,2,4-triazole are presented in Figure 4. DTA thermogram of control 1,2,4-triazole showed two endothermic peaks at 121.98°C and 210.42°C. The first endothermic peak was corresponded to melting temperature and second was due to thermal decomposition of the sample. DTA thermogram of treated 1,2,4-triazole also showed two endothermic peaks at 123.15°C and 222.93°C. The former peak was due to melting temperature of the treated 1,2,4-triazole and latter peak was corresponded to thermal decomposition of the sample. DTA showed an increase in decomposition temperature of treated 1,2,4-triazole with respect to control.

Derivative thermo gravimetry (DTG) thermogram of control 1,2,4-triazole showed maximum thermal decomposition temperature

Parameter	Control	Treated
Latent heat of fusion ΔH (J/g)	132.51	160.55
Melting temperature (°C)	123.76°C	124.22 °C
Tmax (°C)	199.68 °C	213.40 °C
Weight loss (%)	53.79	50.70

Table 2: Thermal analysis data of control and treated 1,2,4-triazole.

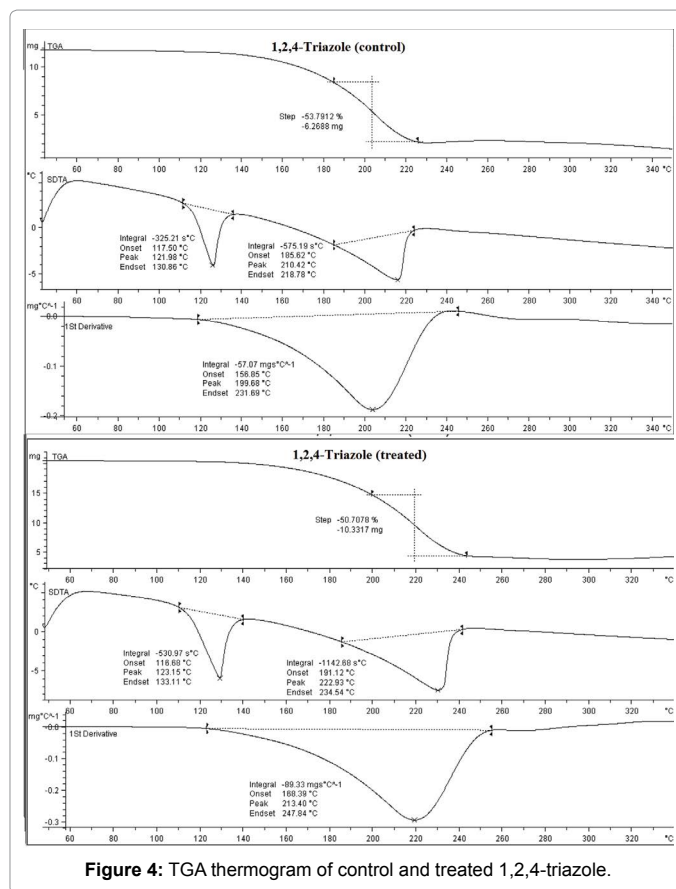


Figure 4: TGA thermogram of control and treated 1,2,4-triazole.

(T_{max}) at 199.68°C and it was increased substantially to 213.40°C in treated 1,2,4-triazole. The result showed 6.87% increase in T_{max} of treated 1,2,4-triazole as compared to control sample. Overall, the increase in onset temperature, and T_{max} corroborated the high thermal stability of treated compound as compared to control 1,2,4-triazole. According to Boltzman law of energy distribution among molecules at any temperature a portion of molecules will possess energy higher than the bond energy.

$$K=Ae^{-E/RT}$$

Where, A is the frequency factor related to vibration frequency of a critical mode of vibration in molecules and E is the excess energy which must be concentrated in the molecule in order to decompose it. K is the rate of decomposition. In this equation temperature (T) is inversely proportional to rate of thermal decomposition (K). Similarly in this work rate of decomposition was decreased with increasing temperature and increase in thermal stability. Additionally, it was reported that A should be minimized in order to increase the thermal stability of the organic compounds [27]. Hence, it is assumed that biofield treatment may be acted on the treated 1,2,4-triazole and minimized the frequency of critical mode of vibration of molecules that leads to increase in thermal stability of treated sample with respect to control.

Surface Area Analysis

The surface area of control and treated 1,2,4-triazole were evaluated using BET analyzer and results are presented in Figure 5. The control 1,2,4-triazole showed a surface area of 0.3802 m²/g and it was increased considerably to 0.4316 m²/g in treated sample. The result showed an increase in surface area by 13.52% with respect to control. The possible

cause of an increase in surface area of treated 1,2,4-triazole could be the decrease in particle size of 1,2,4-triazole after biofield treatment. It was reported that decrease in particle size increases the surface area and vice versa [28,29]. Biofield treatment may provide energy milling which led to the formation of grain into sub grain that caused decrease in particle size and increase in surface area [30].

FT-IR spectroscopy

FT-IR spectra of control and treated 1,2,4-triazole (T1 and T2) samples are presented in Figure 6. The FT-IR spectrum of control 1,2,4-triazole showed characteristic absorption peaks at 3097 and 3032 cm^{-1} due to C-H aromatic vibrations. Vibration peak at 3126 cm^{-1} was due N-H stretching of the sample. FT-IR peaks at 1529 and 1483 cm^{-1} were corresponded to C=C stretching for aromatic groups. Vibration peak for -N=N stretching was observed at 1543 cm^{-1} [31]. Likewise, the FT-IR spectrum of 1,2,4-triazole (T1) showed absorptions peaks at 3095, and 3034 cm^{-1} that were due to C-H aromatic vibrations. N-H stretching vibration was observed at 3128 cm^{-1} in the sample. FT-IR peaks observed at 1529, and 1483 cm^{-1} were corresponded to C=C (aromatic) stretching vibration peak (Figure 6). Vibration peak for -N=N stretching was observed at 1543 cm^{-1} . FT-IR spectrum of 1,2,4-triazole (T2) showed absorption peaks at 3028 cm^{-1} that were due to C-H (aromatic) stretching vibrations. N-H stretching vibration peak was observed at 3128 cm^{-1} in the sample. C=C (aromatic) stretching vibrations were observed at 1529, and 1481 cm^{-1} . N=N stretching peak

was observed at 1543 cm^{-1} in the sample. Overall, the FT-IR results showed no significant structural changes in treated 1,2,4-triazole (T1 and T2) with respect to control sample.

Conclusions

XRD results showed a reduction in unit cell volume and molecular weight of treated 1,2,4-triazole as compared to control. A substantial decrease in crystallite size was evidenced in treated 1,2,4-triazole that may be due to compressive stress caused through biofield treatment with respect to control. DSC characterization showed a slight increase in melting temperature with respect to control. A significant increase in latent heat of fusion was observed in treated 1,2,4-triazole than the control sample. TGA showed a substantial increase in T_{max} of treated compound as compared to control. This indicated the increase in thermal stability of 1,2,4-triazole after biofield treatment. The surface area was increased considerably in treated sample that may improve the solubility of the compound with respect to control. However, no significant change was found in FT-IR absorption peaks of treated 1,2,4-triazole in comparison with control. Based on results it was found that biofield treatment has significantly influenced the physical and thermal properties of treated 1,2,4-triazole. It is assumed that treated 1,2,4-triazole could be used for synthesis of pharmaceutical compounds.

Acknowledgement

Authors thank Dr. Cheng Dong of NLSG, institute of physics, and Chinese academy of sciences for permitting us to use Powder X software for analyzing XRD results. The authors would also like to thank Trivedi Science, Trivedi Master Wellness and Trivedi Testimonials for their support during the work.

References

1. Kucukguzel SG, Suzgun PC (2015) Recent advances bioactive 1,2,4-triazole-3-thiones. *Eur J Med Chem* 97: 830-870.
2. Rezaei Z, Khabnadideh S, Pakshir K, Hossaini Z, Amiri F, et al. (2009) Design, synthesis, and antifungal activity of triazole and benzotriazole derivatives. *Eur J Med Chem* 44: 3064-3067.
3. Gaikwad ND, Patil SV, Bobade VD (2012) Synthesis and biological evaluation of some novel thiazole substituted benzotriazole derivatives. *Bioorg Med Chem Lett* 22: 3449-3454.
4. Wu YS, Lee HK, Li SF (2001) High performance chiral separation of fourteen triazole fungicides by sulfated beta-cyclodextrin mediated capillary electrophoresis. *J Chromatogr A* 912: 171-179.
5. Kumamoto T, Toyooka K, Nishida M, Kuwahara H, Yoshimura Y, et al. (1990) Effect of 2,4-dihydro-3H-1,2,4-triazole-3-thiones and thiosemicarbazones on iodide uptake by the mouse thyroid: the relationship between their structure and anti-thyroid activity. *Chem Pharm Bull (Tokyo)* 38: 2595-2596.
6. Scholz I, Oberwittler H, Riedel KD, Burhenne J, Weiss J, et al. (2009) Pharmacokinetics, metabolism and bioavailability of the triazole antifungal agent voriconazole in relation to CYP2C19 genotype. *Br J Clin Pharmacol* 68: 906-915.
7. Torres HA, Hachem RY, Chemaly RF, Kontoyiannis D, Raad II (2005) Posaconazole: a broad-spectrum triazole antifungal. *Lancet Infect Dis* 5: 775-785.
8. Kurtzer F, Katritzky AR, Boulton AJ (1965) *Advances in Heterocyclic Chemistry*. Academic Press, New York.
9. Blessy M, Patel RD, Prajapati PN, Agrawal YK (2014) Development of forced degradation and stability indicating studies of drugs - A review. *J Pharm Anal* 4: 159-165.
10. Mohammadi H, Hassanzadeh A, Khodabakhsh R (2010) The effect of fast neutron and gamma irradiation on thermal, structural and colorant properties of 2,6-diaminopyridine. *Appl Radiat Isot* 68: 1884-1891.
11. Trivedi MK, Patil S, Shettigar H, Bairwa K, Jana S (2015) Effect of biofield treatment on spectral properties of paracetamol and piroxicam. *Chem Sci J* 6: 98.

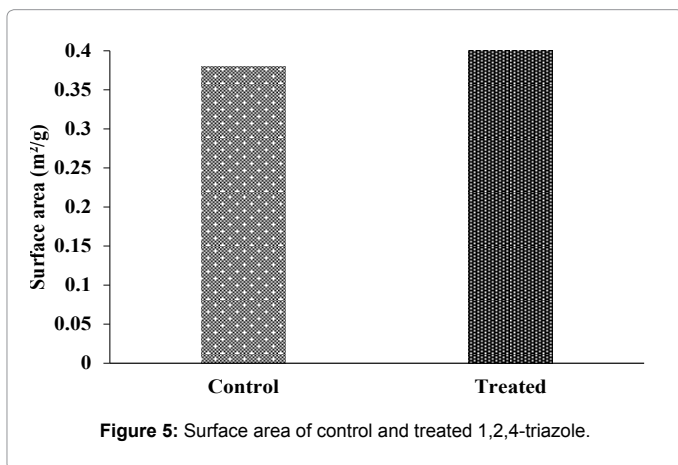


Figure 5: Surface area of control and treated 1,2,4-triazole.

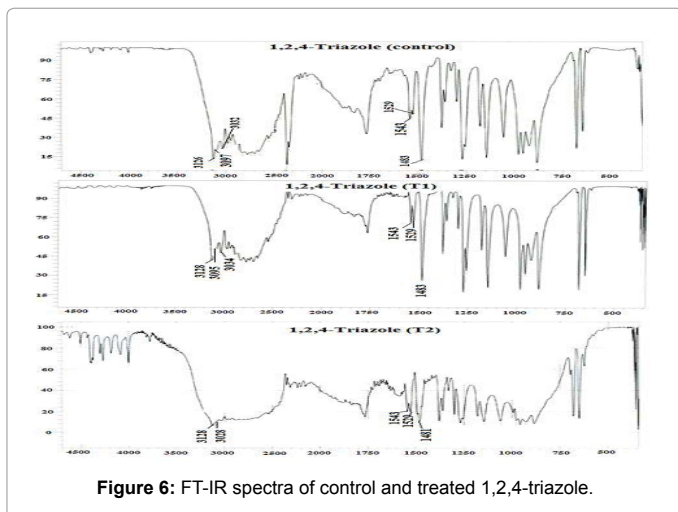


Figure 6: FT-IR spectra of control and treated 1,2,4-triazole.

12. Trivedi MK, Patil S, Tallapragada RM (2013) Effect of bio field treatment on the physical and thermal characteristics of silicon, tin and lead powders. *J Material Sci Eng* 2: 125.
13. Trivedi MK, Nayak G, Patil S, Tallapragada RM, Jana S, et al. (2015) Bio-field treatment: An effective strategy to improve the quality of beef extract and meat infusion powder. *J Nutr Food Sci* 5: 389.
14. Rivera-Ruiz M, Cajavilca C, Varon J (2008) Einthoven's string galvanometer: The first electrocardiograph. *Tex Heart Inst J* 35: 174-178.
15. Shinde V, Sances F, Patil S, Spence A (2012) Impact of biofield treatment on growth and yield of lettuce and tomato. *Aust J Basic Appl Sci* 6: 100-105.
16. Sances F, Flora E, Patil S, Spence A, Shinde V (2013) Impact of biofield treatment on ginseng and organic blueberry yield. *Agrivita J Agric Sci* 35: 22-29.
17. Lenssen AW (2013) Biofield and fungicide seed treatment influences on soybean productivity, seed quality and weed community. *Agricultural Journal* 8: 138-143.
18. Patil SA, Nayak GB, Barve SS, Tembe RP, Khan RR (2012) Impact of biofield treatment on growth and anatomical characteristics of *Pogostemon cablin* (Benth.). *Biotechnology*; 11: 154-162.
19. Trivedi MK, Patil S (2008) Impact of an external energy on *Staphylococcus epidermis* [ATCC –13518] in relation to antibiotic susceptibility and biochemical reactions – An experimental study. *J Accord Integr Med* 4: 230-235.
20. Trivedi MK, Patil S (2008) Impact of an external energy on *Yersinia enterocolitica* [ATCC–23715] in relation to antibiotic susceptibility and biochemical reactions: An experimental study. *Internet J Alternative Med* 6: 2.
21. Trivedi MK, Bhardwaj Y, Patil S, Shettigar H, Bulbule A (2009) Impact of an external energy on *Enterococcus faecalis* [ATCC – 51299] in relation to antibiotic susceptibility and biochemical reactions – An experimental study. *J Accord Integr Med* 5: 119-130.
22. Nayak G, Altekhar N (2015) Effect of biofield treatment on plant growth and adaptation. *J Environ Health Sci* 1: 1-9.
23. Ahamed H, Kumar VS (2011) A Comparative study on the milling speed for the synthesis of nano-structured Al 6063 alloy powder by mechanical alloying. *JMMCE* 10: 507-515.
24. Suryanarayana C (2004) Mechanical alloying and milling. Boca Raton, CRC Press, Florida.
25. Trivedi MK, Patil S, Tallapragada RM (2013) Effect of biofield treatment on the physical and thermal characteristics of vanadium pentoxide powders. *J Material Sci Eng S11*: 001.
26. Moore J (2010) Chemistry: The molecular science (4thedn) Brooks Cole.
27. Johns IB, McElhill EA, Smith JO (1962) Thermal stability of organic compounds. *Ind Eng Chem Prod Res Dev* 1: 2-6.
28. Mennucci B, Martinez JM (2005) How to model solvation of peptides? Insights from a quantum-mechanical and molecular dynamics study of N-methylacetamide. I. Geometries, infrared, and ultraviolet spectra in water. *J Phys Chem B* 109: 9818-9829.
29. Bendz D, Tuchsén PL, Christensen TH (2007) The dissolution kinetics of major elements in municipal solid waste incineration bottom ash particles. *J Contam Hydrol* 94: 178-194.
30. Trivedi MK, Nayak G, Patil S, Tallapragada RM, Latiyal O (2015) Studies of the atomic and crystalline characteristics of ceramic oxide nano powders after bio field treatment. *Ind Eng Manage* 4: 161.
31. Goyal, PK, Bhandari A, Rana AC, Jain CB (2010) Synthesis of some 3-substituted -4h-1,2,4-triazole derivatives with potent anti-inflammatory activity. *Asian J Pharm Clin Res* 3: 244-246.